Cross-talk between GlcNAcylation and phosphorylation: Site-specific phosphorylation dynamics in response to globally elevated *O*-GlcNAc

Zihao Wang, Marjan Gucek, and Gerald W. Hart*

Department of Biological Chemistry, Johns Hopkins University School of Medicine, Baltimore, MD 21205-2185

Communicated by M. Daniel Lane, Johns Hopkins University School of Medicine, Baltimore, MD, June 27, 2008 (received for review March 16, 2008)

Protein GlcNAcylation serves as a nutrient/stress sensor to modulate the functions of many nuclear and cytoplasmic proteins. *O*-GlcNAc cycles on serine or threonine residues like phosphorylation, is nearly as abundant, and functions, at least partially, via its interplay with phosphorylation. Here, we describe changes in site-specific phosphorylation dynamics in response to globally elevated GlcNAcylation. By combining sequential phospho-residue enrichment, iTRAQ labeling, and high throughput mass spectrometric analyses, phosphorylation dynamics on 711 phosphopeptides were quantified. Based upon their insensitivity to phosphatase inhibition, we conclude that ≈48% of these phosphorylation sites were not actively cycling in the conditions of the study. However, increased GlcNAcylation influenced phosphate stoichiometry at most of the sites that did appear to be actively cycling. Elevated GlcNAcylation resulted in lower phosphorylation at 280 sites and caused increased phosphorylation at 148 sites. Thus, the cross-talk or interplay between these two abundant posttranslational modifications is extensive, and may arises both by steric competition for occupancy at the same or proximal sites and by each modification regulating the other's enzymatic machinery. The phosphoproteome dynamics presented by this large set of quantitative data not only delineates the complex interplay between phosphorylation and GlcNAcyation, but also provides insights for more focused investigations of specific roles of *O*-GlcNAc in regulating protein functions and signaling pathways.

regulation | signaling | kinase | O-GlcNAc transferase

Enzyme-catalyzed cycling of O-linked β-*N*-acetylglucosamine (*O*-GlcNAc) is observed on serine and threonine side chains of myriad nuclear and cytoplasmic proteins that are involved in almost all aspects of cellular functions. Unlike extracellular complex glycans, which are generally static, *O*-GlcNAc cycles rapidly on regulatory proteins in response to metabolic and environmental signals at rates comparable to phosphorylation (1, 2, 3). *O*-GlcNAc cycles by the combined actions of two highly conserved enzymes, which catalyze the addition (*O*-GlcNAc transferase, or OGT) and removal (β-*N*-glucosaminidase, or *O*-GlcNAcase) of *O*-GlcNAc, respectively. In mammals, OGT exists in different nucleoplasmic, cytoplasmic or mitochondrial isoforms. But, they share the same catalytic domain, which is encoded by one highly conserved gene (4). Similarly, although there are at least two splicing variants of *O*-GlcNAcase, only one mammalian gene encoding *O*-GlcNAcase exists (5). In contrast to phosphorylation, which involves kinases and phosphatases that represent >2% of the human proteome (6), GlcNAcylation appears to be controlled by regulated transient associations of only two evolutionally conserved enzymes together with different targeting/regulatory subunits (1).

Although the mechanisms controlling their cycling appear to be different, in many other respects GlcNAcylation is similar to phosphorylation. GlcNAcylation is abundant on a wide array of proteins, just like phosphorylation. They both alter the functions and binding partners of the target proteins. Both modifications are inextricably linked to cellular metabolism in that their donor substrates are high-energy end products of nutrient metabolism. Both GlcNAcylation and phosphorylation are found on serine and threonine side chains of nucleoplasmic proteins, and are dynamically regulated in response to cellular stimuli. To date, all of the known GlcNAcylated proteins are also phosphoproteins. More interestingly, many proteins are modified by *O*-GlcNAc or *O*-phosphate on the same or at proximal sites. Based on the reciprocal occupancy of *O*-GlcNAc and *O*-phosphate on several well characterized proteins, a "Yin Yang" model hypothesizes that GlcNAcylation and phosphorylation modulate protein functions, in part, by competitively blocking each other's occupancy at given sites (7). This model was further supported by the finding that OGT forms a complex with protein phosphatase 1 catalytic subunits (PP1c). *In vitro* assays showed that phosphopeptides could be concurrently de-phosphorylated and remodified by *O*-GlcNAc by this functional complex (8). However, recent site-mapping studies have identified increasing numbers of *O*-GlcNAc modification sites that are not the same, but are adjacent or even distal to phosphorylation sites (9, 10). Thus, it is clear that even though the regulatory roles of *O*-GlcNAc are related to its interplay with phosphorylation, the binary "Yin Yang" model is overly simplistic and should be replaced with a more comprehensive model that covers different types of interplay between these two posttranslational modifications (for a review, see ref. 1).

Previously, we reported the perturbations of *O*-GlcNAc induced by inhibition of glycogen synthase kinse-3 (GSK-3). Surprisingly, a significant portion of the identified GlcNAcylated proteins showed decreased GlcNAclyation upon inhibition of GSK-3, indicating extensive nonreciprocal interplay between *O*-GlcNAc and *O*-phosphate (11). Here, this study was extended in the opposite direction. By combining sequential enrichment of phosphoresidues and iTRAQ-based quantitative proteomics, we investigated the site-specific phosphorylation dynamics in response to globally elevated *O*-GlcNAc levels by inhibition of *O*-GlcNAcase. The large set of quantitative data generated in this study illustrates that the complex interplay between these two posttranslational modifications is extensive, and provides insights for future studies of *O*-GlcNAc function on individual proteins and in specific signaling pathways.

Results

Initial Assessment of GlcNAcylation-Phosphorylation Interplay by Immunoblotting. Okadaic acid (OA), a potent inhibitor of serine/threonine-specific protein phosphatases, was used to elevate global phosphorylation levels. Two widely used inhibitors of *O*-GlcNAcase are PUGNAc (*O*-(2-acetamido-2-deoxy-d-glucopyranosylidene)

Author contributions: Z.W. and G.W.H. designed research; Z.W. and M.G. performed research; Z.W. and G.W.H. analyzed data; and Z.W. and G.W.H. wrote the paper.

Conflict of interest statement: G.W.H. receives a share of royalty received by the university on sales of the CTD 110.6 antibody. Terms of this arrangement are managed by Johns Hopkins University School of Medicine.

*To whom correspondence should be addressed. E-mail: gwhart@jhmi.edu.

This article contains supporting information online at www.pnas.org/cgi/content/full/0806216105/DCSupplemental.

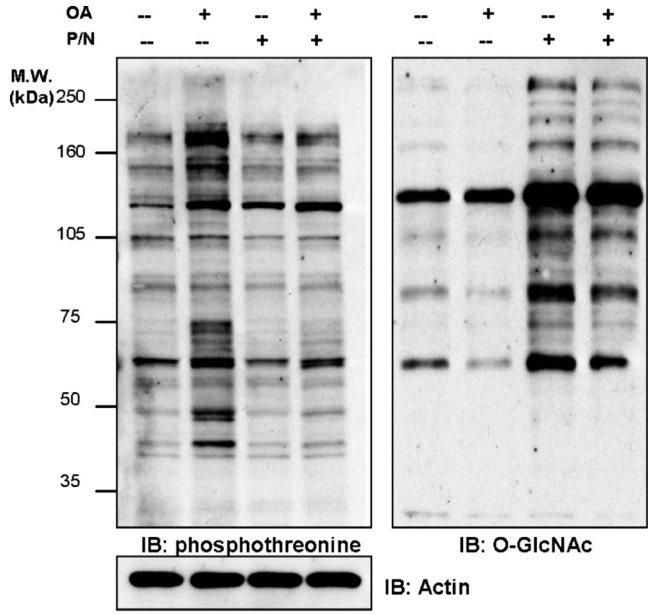

Fig. 1. Effects of elevated GlcNAcylation and phosphorylation on each other. NIH 3T3 cells were untreated and treated with okadaic acid (225 nM), PUGNAc (100 μM), and 20 μM NAG-thiazoline as indicated for 2.5 h before harvest. Cell lysates (20 μg for each group) were resolved in SDS/PAGE, transferred, and blotted with phosphothreonine or *O*-GlcNAc antibody. The same membrane was stripped and blotted with anti-actin for loading control. OA, okadaic acid; P/N, combined treatment with PUGNAc and NAG-thiazoline.

amino-N-phenylcarbamate) and NAG-thiazoline (1, 2-dideoxy-2′-methyl-alpha-d-glucopyranoso [2,1-d]-Delta2′-thiazoline; NAG-T), which significantly increase nucleocytoplasmic *O*-GlcNAc levels after being added to cultured cells (12). In this study, NIH 3T3 cells were treated with OA, PUGNAc and NAG-thiazoline, or all three inhibitors simultaneously. Dynamic changes in GlcNAcylation and phosphorylation were initially evaluated by immunoblotting with antibodies against *O*-GlcNAc and phosphothreonine. Based on results from a time course study (data not shown), 2.5 h of treatment was chosen for the proteomics study, because treating cells for relatively short time by *O*-GlcNAcase inhibitors ensured that stress responses, which might trigger unexpected changes of phosphorylation (3), were not yet initiated. Moreover, a brief treatment avoided potential inhibition of lysosomal hexosaminidases (12). However, a 2.5-h time course is long enough for okadaic acid to elevate phosphorylation on rapidly cycling phosphorylation sites. As shown in Fig. 1, 2.5 h of treatment by PUGNAc/NAG-T induced significantly elevated global GlcNAcylation levels (Fig. 1 *Right*, lane 3 vs. lane 1), whereas OA significantly increased overall threonine phosphorylation (Fig. 1 *Left*, lane 2 vs. lane 1). Changes of threonine phosphorylation patterns in PUGNAc/NAG-T treated cells (Fig. 1 *Left*, lane 3 vs. lane 1) and changes of GlcNAcylation patterns in OA treated cells (Fig. 1 *Right*, lane 2 vs. lane 1) were clearly visible. Also, PUGNAc/NAG-T slightly blunted the increases of threonine phosphorylation induced by OA (Fig. 1 *Left*, lane 4 vs. lane 2). Similarly, OA dampened the increases in GlcNAcylation (Fig. 1 *Right*, lane 4 vs. lane 3) induced by PUGNAc/NAG-T. Pretreatment of the samples with alkaline phosphatase abolished immunoblotting signals, indicating the specificity of the phosphothreonine antibody [supporting information (SI) Fig. S1]. Initial evaluation of serine phosphorylation by immunoblotting was not possible due to lack of phosphoserine antibody with enough specificity.

Sequential Phosphoresidue Enrichment by Combined IMAC and TiO_2. Immunoblotting with pan-specific *O*-phosphate and *O*-GlcNAc antibodies have limited power for assessment of phosphorylation

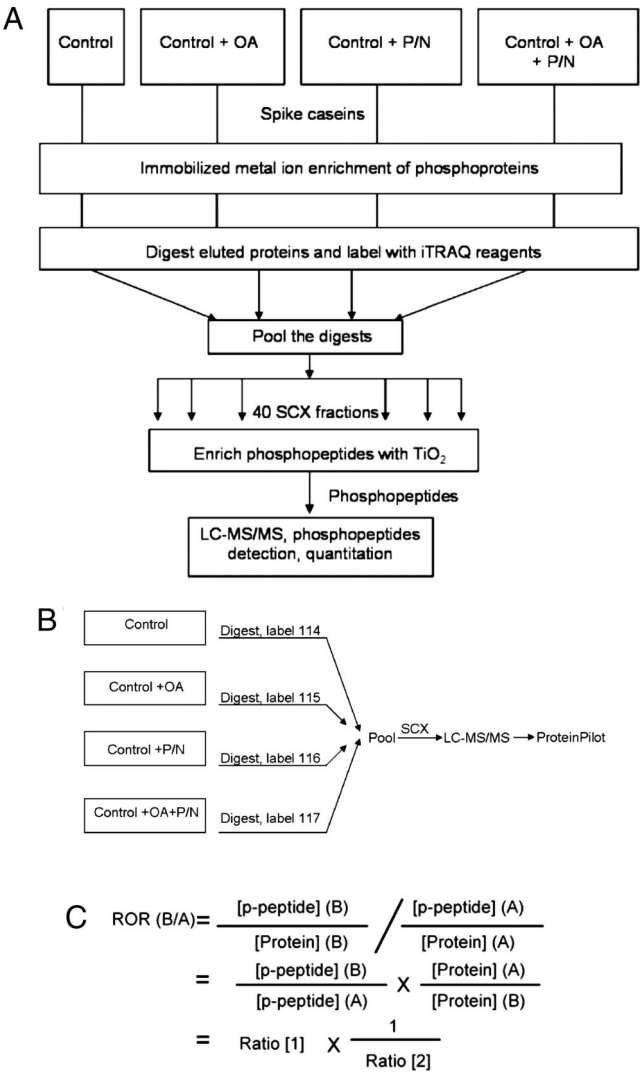

Fig. 2. Quantitative proteomics approach used to delineate global interplay between phosphorylation and GlcNAcylation. (*A*) Flow chart for phosphosite detection and site-specific quantitation. (*B*) Flow chart for protein expression level quantitation using iTRAQ. (*C*) Formula used to calculate RORs.

and GlcNAcylation dynamics because only limited bands could be detected (Fig. 1). Moreover, the immunoblotting approach can only detect changes of overall levels of modification. It is well known that many phosphoproteins are phosphorylated at multiple sites with each site being regulated by different mechanisms and involved in different signaling pathways. Phosphorylation changes at each site may not be clearly detectable at the global level, even though the change at that site may be very significant. Thus, we designed and adopted a proteomics approach to investigate site-specific cross-talk between phosphorylation and GlcNAcylation (Fig. 2*A*). Extensive fractionation and specific enrichment are essential for analyzing the phosphoproteome by mass spectrometry. In the current study, phosphoresidues were sequentially enriched by IMAC (*i*mmobilized *m*etal *a*ffinity *c*hromatography) at the protein level and by titanium dioxide at the peptide level. IMAC is based on the affinity of metals to negatively charged phosphate groups. Using an in-house packed column, phosphoproteins were enriched from NIH 3T3 cell lysates. Caution was taken to ensure that the IMAC columns were not saturated. The yields were ≈5% of the starting materials (Fig. S2). This step also served to reduce the complexity of whole cell lysates. After

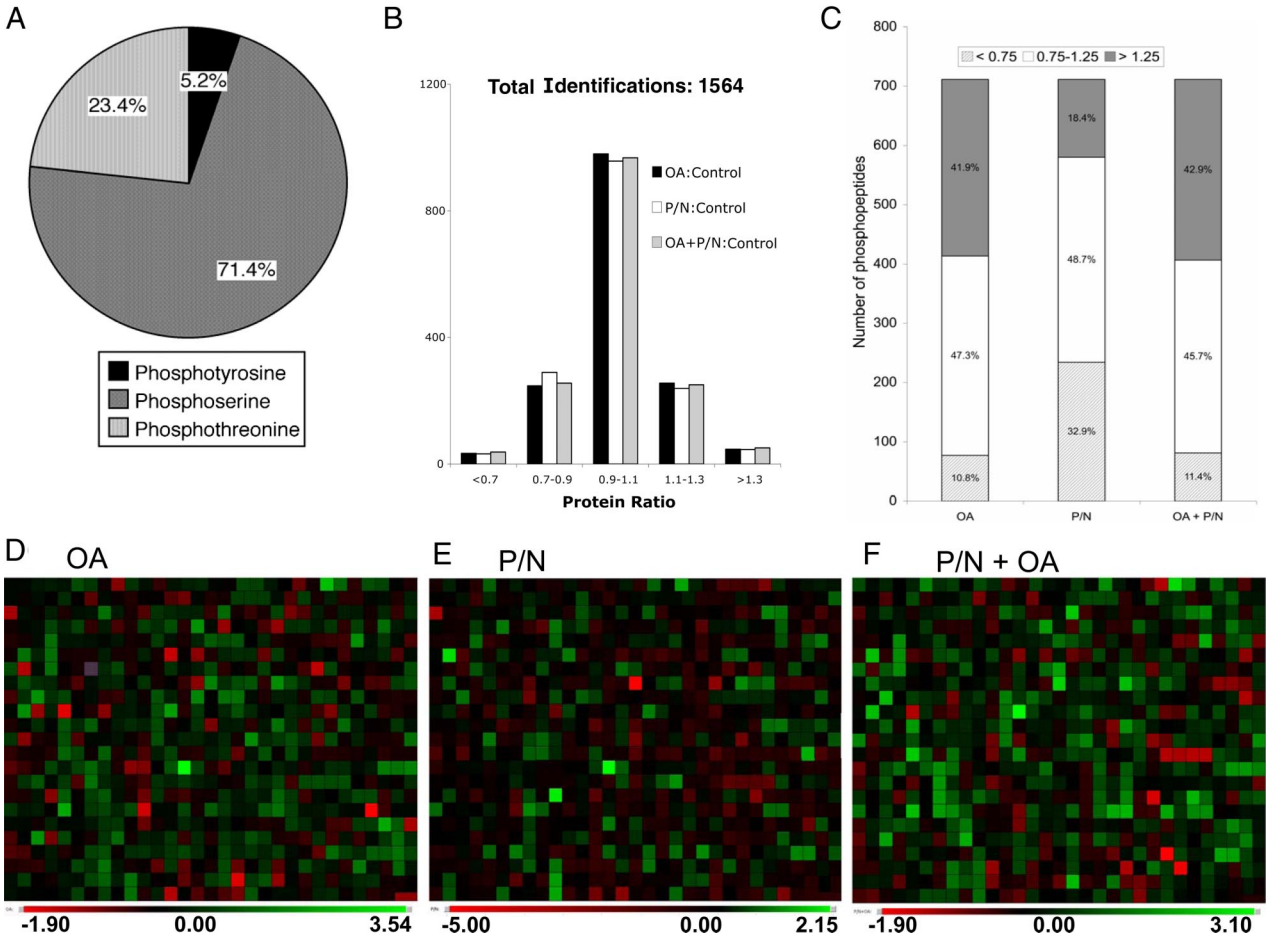

Fig. 3. Summary of large-scale identification and quantitation. (*A*) Distribution of detected phosphoserine, threonine, and tyrosine sites. (*B*) Total number of identified proteins and distribution of protein expression level dynamics. (*C*) Distribution of phosphorylation ROR dynamics. (*D–F*) Log_2 ratios of site-specific phosphorylation RORs under indicated conditions. Positions at the heat maps correspond to the same phosphorylation sites.

IMAC, phosphoproteins were digested, labeled with iTRAQ reagents, and then fractionated by strong cation exchange (Fig. S3), which not only removed excessive iTRAQ reagents but also further enriched phosphopeptides in the first few strong cation exchange fractions (first 12–13 fractions of 40 for this study) because of reduced surface charges of phosphopeptides compared with naked peptides (13). Capillaries packed in-house with TiO_2 beads were used to purify phosphopeptides from each strong cation exchange fraction. Nonspecific binding was reduced by adding 1 M glycolic acid in the loading and washing buffers. Effectiveness of this step was validated in advance by successfully enriching phosphopeptides (EVVG**p***S*AEAGVDAASVSEEFR, and LPGFGD**p***S*IEAQCG-TSVNVHSSLR) from tryptic digest of chicken ovalbumin (data not shown).

Protein Level Quantitation by iTRAQ. The apparent dynamics of phosphorylation may partially result from changes of protein expression levels because of altered transcription, translation, or protein degradation. To address this issue, protein level dynamics were quantified by iTRAQ-based proteomics methods. The amine-specific iTRAQ reagents enabled isobaric tagging of peptides (mostly on the N-term and Lys residues). Intensities of the reporter ions (*m/z* 114.1, 115.1, 116.1, and 117.1) generated from the iTRAQ tags upon fragmentation were used for quantitation. Briefly, equal amounts of cell lysates from each experimental condition were reduced, alkylated, and digested. Resulting peptides were labeled with the 4-plex iTRAQ reagents and pooled. After fractionation by strong cation exchange, peptides were analyzed by using a Q-Star mass spectrometer (Fig. 2*B*). With the threshold of at least one unique peptide with >95% confidence, a total number of 1564 proteins were identified (Table S1). Relative quantitation was automated by using the ProteinPilot software. Manual inspection was performed to exclude peptides with reporter ion intensities exceeding 2,000 counts for quantitation, in which case, the MS detector was likely saturated. Quantitation results showed that relative protein ratios of ≈62% identified proteins fell in the range 0.9–1.1 between all three experimental conditions and the control, and ≈95% were within the range 0.7–1.3 (Fig. 3*B*), indicating that brief treatment by the inhibitors did not lead to significant changes in protein expression levels.

Phosphopeptide Identification, Quantitation, and Global Cross-Talk Between Phosphorylation and GlcNAcylation. Enriched phosphopeptides from each strong cation exchange fraction were analyzed by LC-MS/MS. Database search together with manual interpretation (see *Materials and Methods*) identified and validated 851 novel or previously known phosphosites, including 44 pTyr (5.2%), 608 pSer (71.4%), and 199 pThr sites (23.4%), originating from 351 proteins (Fig. 3*A*). The identified phosphosites originated from proteins involved in an array of biological functions, including cytoskeleton regulatory proteins, metabolic enzymes, kinases, transcription factors, and RNA processing proteins (Table S2). Examples of some identified phosphopeptides are shown in Fig. 4. The false positive rate was estimated to be ≈0.4% by performing a Mascot search

BIOCHEMISTRY

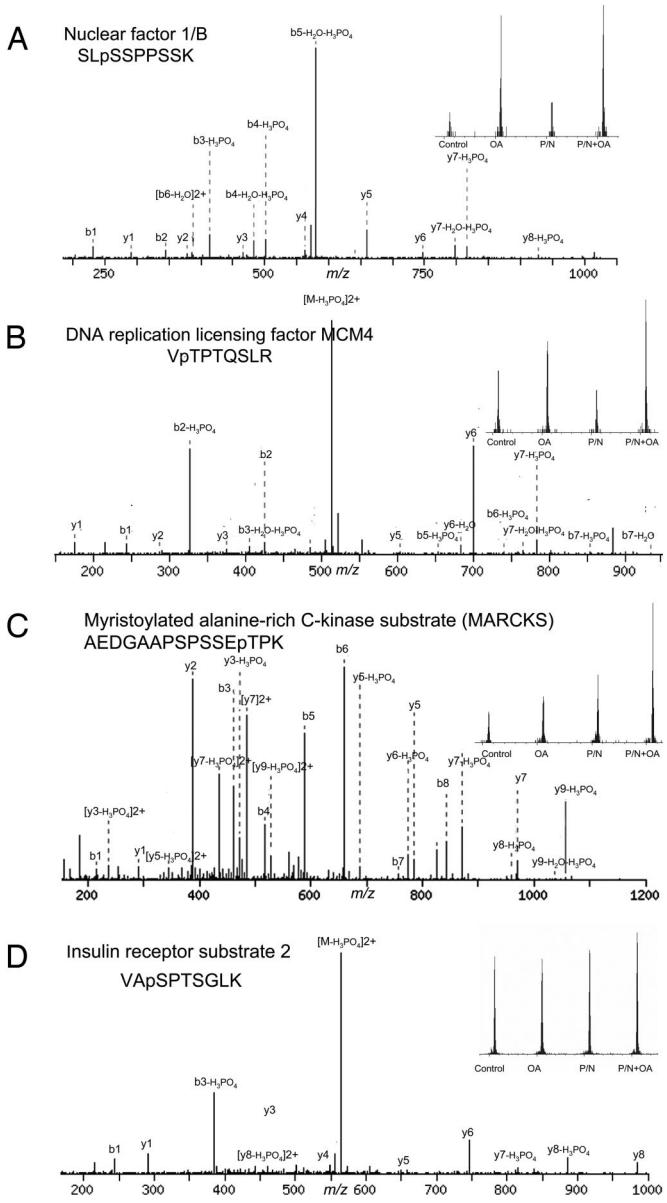

Fig. 4. Detection and quantitation of phosphopeptides. Selected samples originating from nuclear factor 1/B (*A*), DNA replication licensing factor MCM4 (*B*), myristoylated alanine-rich C-kinase substrate (*C*), and insulin receptor substrate 2 (*D*). (*Insets*) Indicate the intensities of iTRAQ reporter ions.

using the same set of parameters but against a reverse database. The Mascot result file was exported and used as one of the input files for MultiQ software (14), which performed phosphopeptide quantitation. For iTRAQ experiment that quantified protein expression levels, systematic bias (pipetting inaccuracy, variation of column elution efficiency, etc) was automatically corrected by the quantitation software, under the assumption that most protein levels were not changed. For experiments that quantified phosphopeptide dynamics, this assumption might not be valid. To address this issue, an internal standard was applied for quantitation. Equal amounts of bovine α- and β-caseins (0.05 μg of each) were spiked into samples from the very beginning. After MS analyses, 25 phosphopeptides originating from caseins were identified, 21 of which were also quantified (Fig. S4). The weighed average ratios of these phosphopeptides were calculated and used as an internal standard, to which all other ratios were normalized.

Relative fold changes were obtained from 711 phosphopeptides and normalized to the internal standard for bias correction. Technical duplicates were performed under the same experimental conditions. The average relative standard deviation (%RSD) was estimated to be <24%. Of the 351 corresponding phosphoproteins, 207 were also identified and quantified in the iTRAQ experiment designed for protein level quantitation. With relative ratios of both phosphopeptides and whole proteins available, relative occupancy ratios (RORs) of *O*-phosphate were calculated by using a simple formula (Fig. 2*C*), which better reflected the actual dynamic changes of phosphorylation at each specific site, and were thus more biological meaningful. RORs of phosphopeptides originating from the remaining 144 phosphoproteins were similarly calculated assuming the protein ratios were 1:1:1:1 because levels of most proteins were not changed (Fig. 3*B*) during short exposure to the inhibitors. Numbers of phosphopeptides with RORs falling in each fold change category in response to inhibitor treatments are shown in Fig. 3*C*. In summary, after OA treatment, 298 of 711 (41.9%) peptides showed significantly increased phosphate RORs and 77 (10.8%) peptides showed decreased RORs. After PUGNAc/NAG-T treatment 234 (32.9%) peptides showed significantly decreased phosphate RORs, and 131 (18.4%) peptides showed increased RORs. In both cases, ≈48% peptides did not show significant changes in phosphate RORs, indicating that they are likely not cycling. Samples treated by both phosphatase and *O*-GlcNAcase inhibitors exhibited a similar pattern of phosphorylation dynamics as samples treated by phosphatase inhibitor alone. The "significant" fold change thresholds (0.75 and 1.25) were chosen based on quantitation %RSD (< 24%) estimated from technical duplicates. The relative ratios of site-specific phosphorylation RORs under different conditions appear as heat maps in Fig. 3 *D–F*. The green scale bar that represents up-regulated phosphorylation is bigger in Fig. 3*D* than in Fig. 3*F*, reflecting attenuated increases of phosphorylation by okadaic acid when cells were simultaneously treated by PUGNAc and NAG-thiazoline, which is in agreement with immunoblotting results (Fig. 1).

GlcNAcylation/Phosphorylation Interplay on Proteins from Different Functional Groups. Earlier studies suggested potentially different patterns of cross-talk between the two posttranslational modifications on proteins that are involved in different biological processes or that have different subcellular localizations (11). Thus, we investigated whether such differences could also be seen in the current more comprehensive and quantitative study. Information about the functions and subcellular localization of the identified phosphoproteins were obtained from existing public databases (see *Materials and Methods*) and included in Table S2. Upstream kinases responsible for 250 phosphosites were also indicated, including 49 experimentally known and 201 predicted by SCANSITE algorithm with high stringency (Table S2). Patterns of GlcNAcylation/phosphorylation interplay on proteins from two major functional groups are presented in Fig. 5. One group included cytoskeleton and cytoskeleton-binding proteins that are localized in the cytoplasm, for which the dynamics of 113 phosphosites were examined. The other group included RNA- and DNA-binding proteins, which are mostly localized in the nucleus, and the dynamics of 208 phosphosites were examined. Reciprocal interplay was more predominately observed on phosphopeptides originating from cytoskeleton and cytoskeleton-binding proteins. Furthermore, we compared the effects of *O*-GlcNAcase inhibitors on the phosphodynamics of substrates of two distinct kinases, CDC2 and casein kinase 2, the two kinases with largest groups of identified substrates in this study (27 entries for CDC2, 10 experimentally known; 28 entries for CK2, all SCANSITE prediction) (Fig. S5). No apparent difference in patterns was observed.

Discussion

This study provides clear quantitative documentation on the interplay between GlcNAcylation and phosphorylation at the individual site

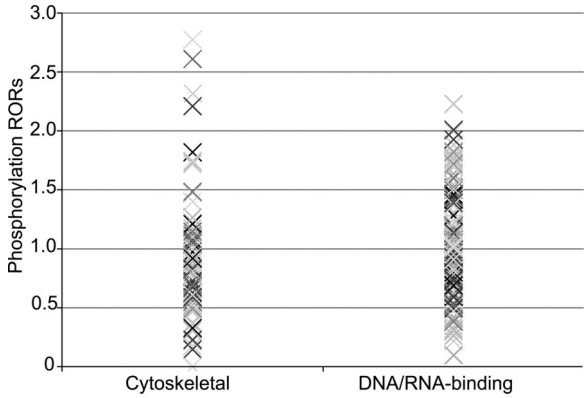

Fig. 5. DNA/RNA-binding proteins showed different patterns of phosphorylation dynamics after treatment of *O*-GlcNAcase inhibitors compared with cytosketetal and cytoskeleton-binding proteins.

level. An advantage of current approach is that it allowed quantification of site-specific phosphorylation dynamics at hundreds of sites in the same experiment. Indeed, many phosphoproteins are modified at multiple sites with each site involved in different pathways and responded differentially to elevated GlcNAcylation (Table S2).

Cross-talk or interplay between GlcNAcylation and phosphorylation may arise from the following mechanisms: (*i*) Direct competition for site-occupancy at a single hydoxyl group. 2) Competition via steric hindrance by reciprocal modification at proximal sites on a polypeptide. 3) Regulation of *O*-GlcNAc Transferase or *O*-GlcNAcase by phosphorylation of their catalytic subunits or of their regulatory/targeting subunits. 4) Regulation of kinases or phosphatases by GlcNAcylation.

As expected, okadaic acid treatment led to increased phosphorylation on ≈42% of the phosphosites. Surprisingly, OA also caused decreased phosphorylation on a small number of phosphosites (≈11%). This might be due to some indirect mechanisms, such as inhibition of corresponding upstream kinases or by increased activation of OGT due to its hyperphosphorylation. In contrast, treatment by *O*-GlcNAcase inhibitors induced decreased phosphorylation on ≈33% of phosphosites and increased phosphorylation on ≈18% of phosphosites. In both samples, no significant phosphorylation dynamics were observed on ≈48% phosphosites, which might corresponded to static or slow-cycling phosphate moieties. For samples treated by both phosphatase and *O*-GlcNAcase inhibitors, the phosphorylation dynamics profile was similar to that of samples treated by phosphatase inhibitor alone. This may not be surprising, because unlike OA, which directly inhibits phosphate removal, *O*-GlcNAc inhibitors cause phosphorylation perturbations by indirect mechanisms. The observation that a large portion of peptides showed decreased phosphorylation upon *O*-GlcNAcase inhibition, suggests that at these sites a competitive relationship does exist. However, the observed reciprocal dynamics do not necessarily result from reciprocal occupancy of the two modifications at the same sites. Indeed, because many signaling cascades occur in a time scale of seconds to minutes, 2.5-h time course of inhibitor treatment allows enough time for secondary effects to contribute the observed reciprocal dynamics. Also, ≈18% of the phosphosites showed increased phosphorylation upon *O*-GlcNAcase inhibition, indicating existence of the nonreciprocal interplay.

As summarized above, underlying mechanisms as to how increased GlcNAcylation might alter phosphorylation dynamics could be as follows: First, competitive occupancy of *O*-GlcNAc and *O*-phosphate occurs at the same sites on some phosphoproteins, for example Thr-58 of transcription factor c-Myc (15), Ser-1177 of endothelial nitric oxide synthase (16), and Ser-16 of murine estrogen receptor-β (17), and others (1). However, because of limited numbers of known *O*-GlcNAc sites, it is presently unclear how prevalent this direct competition for site occupancy actually is. In fact, recent site-mapping reports showed that most of the identified phosphorylation sites and GlcNAcylation sites were at different locations from rat brain postsynaptic density preparations (10, 18). Second, cycling of phosphorylation is affected by adjacent or proximal *O*-GlcNAc moieties due to steric hinderance. For example, GlcNAcylation of Ser-149 on tumor suppressor p53 decreases phosphorylation at Thr-155 (19). It should be noted that cases of adjacent occupancy include not only adjacent modification sites on the primary amino acid sequence, but also distant modifications that are brought close after protein folding. Third, *O*-GlcNAc modification may regulate phosphorylation by altering target proteins' binding to regulatory partners, such as kinases and cofactors. Earlier evidence suggested that *O*-GlcNAc moieties recruited proteins with lectin-like characteristics to the modified proteins (20). Fourth, *O*-GlcNAc and *O*-phosphate interplay by compartmentalizing or directly regulating activities of each other's upstream enzymes (e.g., OGT and kinases). As reported earlier, OGT is activated by CaMKIV-dependent phosphorylation upon depolarization in neuroblastoma cells (21). Likewise, GlcNAcylation affects specific kinase activities (Dias *et al.*, unpublished). The observed phosphorylation dynamics in the current study may reflect the cells' strategies to cope with globally elevated O-GlcNAcylation. The prevalence and magnitude of the cross-talk between GlcNAcylation and phosphorylation clearly supports the importance of the subtle balance between phosphorylation and GlcNAcylation. It has been suggested that tipping this balance to favor increased GlcNAcylation contributes to glucose toxicity and perhaps to insulin resistance, both hallmarks of diabetes (22). Another well known example is the microtubule protein tau, in which disruption of the balance to favor hyperphosphorylation contributes to tangle formation and to Alzheimer's disease (23).

The sensitivity of GlcNAcylation to virtually all aspects of cellular metabolism and its dynamic cycling on and off regulatory proteins makes the modification ideally suited to be a nutrient/stress sensor (3). The involvement of *O*-GlcNAc in signaling pathways includes altering subcellular localization of signaling molecules, regulating cellular responses to insulin, stress protection, cell cycle control, and perhaps most importantly regulating gene transcription (for review, see (2)). The roles of *O*-GlcNAc in cellular signaling are at least in part due to its complex interplay with phosphorylation. In the current study, inhibition of *O*-GlcNAcase led to differentially regulated phosphorylation on many signaling molecules. Significantly decreased phosphorylation was observed at Ser-243 of glucosamine-fructose-6-phosphate aminotransferase (GFAT), the rate limiting enzyme in the hexosamine biosynthesis pathway (HBP). Previous studies demonstrated that phosphorylation at a different site (Ser-205, not detected in the current study) was correlated with altered GFAT activity and subsequently altered production of UDP-GlcNAc (24). Because UDP-GlcNAc is the donor substrate for OGT, it is possible that an unknown feedback inhibition mechanism exits, which involves Ser-243 phosphorylation of GFAT to further regulate flux through the HBP.

Previously, by using stable isotope labeling by amino acid in cell culture (SILAC)-based quantitative proteomic approach, we reported *O*-GlcNAc dynamics in response to inhibition of GSK-3 kinase. Most cytoskeleton-related proteins showed increased GlcNAcylation, whereas most RNA-processing proteins showed decreased GlcNAcylation upon GSK-3 inhibition (11). Earlier studies by using immunoblotting approaches also showed that changes in phosphorylation, which were induced by manipulating kinase activities, were correlated with reciprocal dynamics of GlcNAcylation on cytoskeletal and cytoskeleton-associated proteins, but not on nuclear proteins (25), although the patterns observed varied in different cell lines (26). Here, we compared patterns of *O*-GlcNAc induced phosphorylation dynamics on phosphosites from two protein functional groups that had the largest sample sizes in our study. Caution was taken to exclude multifunc-

tional proteins. As shown in Fig. 5, reciprocal dynamics between GlcNAcylation and phosphorylation were more predominantly observed on cytoplasm-localized cytoskeleton and cytoskeletal-binding proteins, whereas a more diverse range of cross-talk was observed on nuclear-localized DNA- and RNA-binding proteins, including transcription factors. This might reflect the nature of more complex regulation of the DNA- and RNA-binding proteins. Similarly, we compared patterns of interplay between substrates of two kinases (CDC2 and casein kinase 2) (Fig. S5), but no apparent difference in cross-talk was observed in these respective kinase substrates. This might be due to the limited sample sizes of each substrate group and the fact that many phosphosites are regulated by multiple kinases.

Enrichment of *O*-GlcNAc peptides and direct mapping *O*-GlcNAc sites remained difficult until the recent introduction of chemo-enzymatic tagging approaches (10, 12). These approaches can be easily combined with stable isotope labeling for simultaneous *O*-GlcNAc site-mapping and site-specific *O*-GlcNAc quantitation by mass spectrometry. Applying these approaches to the model described in the current study will not only identify rapidly cycling *O*-GlcNAc modifications on regulatory proteins, but also help further delineate the complex cross-talk between GlcNAcylation and phosphorylation.

Materials and Methods

IMAC, iTRAQ Labeling, and Strong Cation Exchange Chromatography. Fast-flow chelating Sepharose with iminodiacetic acid (IDA) was charged with gallium and packed into columns. Cell lysates were passed through IMAC columns (0.5 cm × 3 cm). Phosphoproteins were eluted with buffer containing 100 mM Na_3PO_4, 500 mM NaCl, and 100 mM EDTA/EGTA). After precipitation, protein pellets were resuspended, digested, and labeled by iTRAQ reagents (Applied Biosystems) according to manufacturer's instruction. Labeled peptides were combined and fractionated by strong cation exchange using a polysulfoethyl A column (PolyLC).

Phosphopeptides Enrichment by TiO_2. TiO_2 was packed into a fritted capillary (100 μm i.d.). Peptides in 80% acetonitrile, 4% TFA, and 1 M glycolic acid, were loaded into the capillary and washed. Phosphopeptides were eluted by NH_4OH (pH 11).

LC and MS. Peptides were analyzed on a QStar Pulsar mass spectrometer (Applied Biosystems-MDS Sciex) coupled with an Eksigent nano-LC system. The main HPLC gradient was 5–40% solvent B (A, 0.1% formic acid; B, 90% acetonitrile, 0.1% formic acid) in 60 min at a flow rate of 300 nl/min. The mass spectrometer was set in data-dependent acquisition mode. A rolling collision energy was used to promote fragmentation and the collision energy was increased by 30% to facilitate generating iTRAQ reporter ions.

Data Analysis and Validation. Identification and quantitation of proteins from whole cell lysates were performed by using the ProteinPilot software, Version 2.0 (Applied Biosystems). MS spectral files obtained from phosphopeptides were combined by MultRawPrepare (an MSQuant tool, http://msquant.sourceforge.net) and searched against SwissProt database by the Mascot algorithm, Version 2.2.0. All identifications and spectra were manually inspected to ensure proper identification and phosphate localization. Phosphopeptide quantitation was performed by MultiQ software, Version 1.5.1. All phosphopeptide quantitation was manually validated for accuracy and to exclude quantitation based on reporter ions with suboptimal signal-to-noise ratios. For details, see *SI Materials and Methods*.

Bioinformatics. Information about function subcellular localization of identified proteins was obtained from the UniProt Knowledgebase (UniProtKB, http://beta.uniprot.org) and the Human Protein Reference Database (www.hprd.org). Assignment of upstream kinases of the identified phosphorylation sites were either based on information from the two databases or by prediction with SCANSITE algorithm (http://scansite.mit.edu).

ACKNOWLEDGMENTS. We thank Dr. Dwella Nelson and Dr. Robert Cotter for discussion about alternative instrumentation. This study involved use of the Johns Hopkins University School of Medicine proteomics core facilities. This work was supported by National Institutes of Health Grant CA42486 and National Institutes of Health Contract N01-HV-28180 (to G.W.H.).

1. Hart G, Housley M, Slawson C (2007) Cycling of O-linked β-N-acetylglucosamine on nucleocytoplasmic proteins. *Nature* 446:1017–1022.
2. Slawson C, Housley M, Hart G (2006) O-GlcNAc cycling: How a single sugar post-translational modification is changing the way we think about signaling networks. *J Cell Biochem* 97:71–83.
3. Zachara N, Hart G (2004) O-GlcNAc a sensor of cellular state: The role of nucleocytoplasmic glycosylation in modulating cellular function in response to nutrition and stress. *Biochim Biophys Acta* 1673:13–28.
4. Kreppel L, Hart G (1999) Regulation of a cytosolic and nuclear O-GlcNAc transferase. Role of the tetratricopeptide repeats. *J Biol Chem* 274:32015–32022.
5. Gao Y, Wells L, Comer F, Parker G, Hart G (2000) Dynamic O-glycosylation of nuclear and cytosolic proteins. Cloning and characterization of a neutral, cytosolic β-N-acetylglucosaminidase from human brain. *J Biol Chem* 276:9838–9845.
6. Manning G, Whyte D-B, Martinez R, Hunter T, Sudarsanam S (2002) The protein kinase complement of the human genome. *Science* 298:1912–1934.
7. Wells L, Voeesller K, Hart G (2001) Glycosylation of nucleocytoplasmic proteins: Signal transduction and O-GlcNAc. *Science* 291:2376–2378.
8. Wells L, Kreppel L, Comer F, Wadzinski B, Hart G (2004) O-GlcNAc transferase is in a functional complex with protein phosphatase 1 catalytic subunits. *J Biol Chem* 279:38466–38470.
9. Khidekel N, Ficarro S, Peters E, Hsieh-Wilson L (2004) Exploring the. O-GlcNAc proteome: Direct identification of O-GlcNAc-modified proteins from the brain Proc Natl Acad Sci USA 101:13132–13137.
10. Vosseller K, *et al.* (2006) O-linked. N-acetylglucosamine proteomics of postsynaptic density preparations using lectin weak affinity chromatography and mass spectrometry Mol Cell Proteomics 5:923–934.
11. Wang Z, Pandey A, Hart G (2007) Dynamic Interplay between. O-Linked N-acetylglucosaminylation and glycogen synthase kinase-3-dependent phosphorylation Mol Cell Proteomics 6:1365–1379.
12. Whitworth G, *et al.* (2007) Analysis of PUGNAc and NAG-thiazoline as transition state analogues for human O-GlcNAcase: Mechanistic and structural insights into inhibitor selectivity and transition state poise. *J Am Chem Soc* 129:635–644.
13. Ballif B, Villen J, Beausoleil S, Schwartz D, Gygi S (2004) Phosphoproteomic analysis of the developing mouse brain. *Mol Cell Proteomics* 3:1093–1101.
14. Yu CY, Tsui YH, Yian YH, Sung TY, Hsu WL (2007) The Multi-Q web server for multiplexed protein quantitation. *Nucleic Acids Res* 35:W707–W712.
15. Kamemura K, Hayes B, Comer F, Hart G (2002) Dynamic interplay between O-glycosylation and O-phosphorylation of nucleocytoplasmic proteins: Alternative glycosylation/phosphorylation of Thr-58, a known mutational hot spot of c-Myc in lymphomas, is regulated by mitogens. *J Biol Chem* 277:19229–19235.
16. Musicki B, Kramer M, Becker R, Burnett A (2005) Inactivation of phosphorylated endothelial nitric oxide synthase (Ser-1177) by O-GlcNAc in diabetes-associated erectile dydfunction. *Proc Natl Acad Sci USA* 102:11870–11875.
17. Cheng X, Cole R, Zaia J, Hart G (2000) Alternative. O-glycosylation/O-phosphorylation of the murine estrogen receptor beta. *Biochemistry* 39:11609–11620.
18. Trinidad J, Specht C, Thalhammer A, Schoepfer R, Burlingame A (2006) Comprehensive identification of phosphorylation sites in postsynaptic density preparations. *Mol Cell Proteomics* 5:914–922.
19. Yang W, *et al.* (2006) Modification of p53 with. O-linked N-acetylglucosamine regulates p53 activity and stability Nat Cell Biol 8:1074–1083.
20. Guinez C, Lemoine J, Michalski J, Lefebvre T (2004) 70-kDa-heat shock protein presents an adjustable lectinic activity towards O-linked N-acetylglucosamine. *Biochem Biophys Res Commun* 319:21–26.
21. Song M, Kim H, Park J, Kim S, Kim I, Ryu S, Suh P (2008) O-GlcNAc transferase is activated by CaMKIV-dependent phosphorylation under potassium chloride-induced depolarization in NG-108015 cells. *Cell Signal* 20:94–104.
22. Vosselller K, Wells L, Lane M-D, Hart G (2002) Elevated nucleocytoplasmic glycosylation by O-GlcNAc results in insulin resistance associated with defects in Akt activation in 3T3–L1 adipocytes. *Proc Natl Acad Sci USA* 99:5313–5318.
23. Liu F, Iqbal K, Grundke-Iqbal I, Hart G, Gong C (2004) O-GlcNAcylation regulates phosphorylation of tau: A mechanism involved in Alzheimer's disease. *Proc Natl Acad Sci USA* 101:10804–10809.
24. Chang Q, Su K, Baker J, Yang X, Paterson A, Kudlow J (2000) Phosphorylation of human glutamine:fructose-6-phosphate amidotransferase by cAMP-dependent protein kinase at serine 205 blocks the enzyme activity. *J Biol Chem* 275:21981–21987.
25. Schmitz B, Griffith L (1999) O-linked N-acetylglucosamine levels in cerebellar neurons respond reciprocally to perturbations of phosphorylation. *Eur J Biochem* 262:824–831.
26. Lefebvre T, *et al.* (1999) Effect of okadaic acid on. O-linked N-acetylglusamine levels in a neuroblastoma cell line. *Biochim Biophys Acta* 1472:71–81.